Applied Mathematics & Information Sciences
An International Journal

The solution of a complex integro differential equation in the right half-plane via an infinite plate weakened by a curvilinear hole

Azhar R. Jan

Mathematics Department, Faculty of Sciences, Umm Al-Qura University, Makkah, Saudi Arabia

Abstract: This paper reports on a new study of a flexible plate reduced by a curvilinear slot with the cavity transported conformally to the right half-plane with complex constant parameters of the rational mapping function. Some figures of the conformal mapping for different values of complex constants were also obtained. Some special and important cases have been derived. Also, a closed form of the two Gaursat functions was derived using the complex variable method for the first and second fundamental problems. This is done by converting the first and second basic equations, in the presence of heat, into an integral differential equation in the right half plane with a Cauchy kernel. In addition, the researcher was able to discuss some important applications while studying the effect of temperature in each case. All calculations and computations of various stress components for each application are performed using the Maple 18 program. This study differs from previously published literature, which had areas mapped identically outside or inside the unit circle.

Keywords: Integro differential equation, stress and strain components, Gaursat functions in the complex plane, conformal mapping, half-plane.

1 Introduction

For panel structural components with multiple holes (cracks) that are subjected to external forces, there is frequently a greater concentration of stress around the holes. Therefore, accurately calculating the edge stresses of the perforations are crucial for evaluating the structural stability and reinforcement of the material. Therefore, there are two varieties of cuts in elastic materials, one of which is called a crack, and the other is called a hole. Both cracks or holes are of scientific significance in the study, as is how to treat them. So, we will first shed light on the definitions of each of them. For a crake's problems, in two-dimensional elasticity, there are two varieties of crakes: in the range [-1, 1]. Moreover, this type produces a variety of integral/integro differential equations with singular inputs in one of the following forms:

(i) The kernel of the integral/ integro differential the equation has a weak singular form, logarithmic kernel $k(\mid x - y \mid) = ln \mid x - y \mid$, Carleman function

$k(\mid x - y \mid) = \mid x - y \mid^{-\alpha}, 0 < \alpha < 1$, and Hilbert kernel $k(\mid x - y \mid) = cot(\frac{\mid x - y \mid}{2})$, in the interval $(\frac{-\pi}{2}, \frac{\pi}{2})$.

(ii) For the kernel $k(\mid x - y \mid) = \frac{1}{(x-y)^m}$ at $m = 1$, we have Cauchy singular kernel. While we have a strong singular kernel at $m = 2$ and a super strong singular kernel at $m > 2$.

These kinds of singular equations are amenable to numerous analytic solutions (for the first kind of singular integral equations) or numerical methods (for the first and second kinds of singular integral equations). For example, in Zachariah et al. [2], an application of Aramid/Carbon fiber-reinforced polymer hybrid thin laminate for enhancing static and dynamic transverse loading behaviour was established and investigated, and its the solution was discussed. Gonenli and Das investigated the effect of fractures on the free vibration response of thin circular and annular plates in [3]. In [4], Lal et al. discussed, using various numerical examples, discontinuities, like voids, soft and hard inclusions of the intensity factor of mode stress, fracture growth and the energy release rate of Abdou et al. [7]-[8] contain

* Corresponding author e-mail: arjaan@uqu.edu.sa

supplementary information on the solution of integral/integro differential equations with singular kernels taking a Cauchy form When the kernel assumes a closed curvilinear hole, a second variety of integral/integro differential equation results. In the sense that the problem is caused by an elastic plate with a curved opening in the complex an edge crack isotropic plate under different loadings. The works of Duruk et al. [5], Jan [6], and plane of the theory of elasticity, there are two possible solutions: the first is to move the curved opening outside the unit circle. Exadaktylos et al. [9]-[10], Lu et al. [11], Abdou [12], Abdou and Asseri [13]-[14], and Zeng and Zhang [15] contain additional information. The second can rotate the aperture within the unit circle. Refer to Abdou and Baseem [16] and Alhazmi et al. [17] for additional information. In the preceding two instances, the potential functions are referred to as Gaursat functions.

In this work, we consider the conformal mapping

$$z = \omega(s) = \frac{l(s+1)^2 + m(s-1)^2}{(s^2-1) - n(s-1)^2}, \quad (1)$$
$$Res > 0, s = \sigma + i\zeta, \mid n \mid, \neq 1.$$

Where, in general $l = l_1 + il_2$, $m = m_1 + im_2$ and $n = n_1 + in_2$ are complex parameters subjected to the condition $\omega(s)$ is a single-valued analytic function in the right half-plane $Res \geq 0$. Moreover $\omega(\infty)$ is bounded and $\omega'(\infty) \neq 0$ within $Res \geq 0$.

For the right half-plane, after using the complex variable technique, the Gaursat functions and stress components will be determined for the fundamental boundary value problems (first and second case) in the thermoelastic plate. This elastic plate with a perforation C will be transformed into the proper half-plane $s = \sigma + i\tau, \parallel s \parallel > 0$ by using the logic mapping function (1) considering the heat flow uniformly in the negative direction of the y-axis. Many special cases have been deduced in which the shape of the opening is an ellipse, a crescent, or a cut in the form of a curved arc. Also, some applications that represent the first and second boundary value problems of the infinitely flexible thermoplastic plate with a curved aperture were studied. Finally, cases of transforming the conformal mapping $z = \omega(\zeta)$ inside or outside the unit circle γ will be constructed.

2 Formulating the problem and its basic equations

Consider a thin plate made of an elastic material that has a thickness h and has a closed hole C of indefinite shape. The points inside the holes are conformally mapped into the part of the right half-plane by the mapping of Equation (1). Consider $\Theta = qy$ is the heat equation that flows uniformly in the negative the direction of the y-axis. Consider the temperature $\Theta(x, y)$ is a constant for the

time. Here, q is the constant temperature gradient. In this case, the uniform flow of heat is dispersed by the presence of an insulated curved cavity C, and the heat equation satisfies the relation:

(i)

$$\nabla^2 \Theta = 0, \nabla^2 = \frac{\partial^2}{\partial x^2} + \frac{\partial^2}{\partial y^2}, \quad (2)$$

(ii) $\frac{\partial \Theta}{\partial r}$, on the boundary $r = r_0, r = x + iy$.

The potential of thermoelastic function satisfies, see Parkus [18]

$$\nabla^2 \Xi = (1+v)\alpha\Theta. \quad (3)$$

Here, α and $v(0 \leq v < 1)$ are the thermal expansion coefficient and Poisson's ratio, respectively. Such a problem in the thermoelastic plate satisfies the first and second boundary conditions; see Parkus [18] and Hetnarski and Ignaczak [19].

$$K\Phi_1(t) - t\overline{\Phi_1'(t)} - \overline{\Psi_1(t)} = F(t). \quad (4)$$

Here K is a constant (will be explained) and $F(t)$ is a given free term. The variable t denotes the affix of the boundary. The two complex potential function $\Phi_1(z)$ and $\Upsilon_1(z)$ are given by

$$\Phi_1(z) = -\frac{S_x + iS_y}{2\pi(1+\kappa)}ln(z) + \Gamma z + \Phi(z), \Psi_1(z)$$
$$= -\frac{\kappa(S_x - iS_y)}{2\pi(1+\kappa)}ln(z) + \Gamma^* z + \Psi(z). \quad (5)$$

Here, in Equation (5) S_x and S_y are the components of all external forces that act on the boundary; Γ and Γ^* are the stresses at infinity. In general, $\Phi(z)$ and $\Psi(z)$ are two single analytic functions, in the right half-plane $Res \geq 0$, and holomorphic at infinity. Finally, κ is the thermal conductivity of the material.

For the first fundamental boundary value problem $K = -1$, $S_x = S_y = 0$, and

$$F(t) = \frac{\partial \Xi}{\partial x} + i\frac{\partial \Xi}{\partial y} + \frac{1}{2G}\int_0^s [iL(s) - D(s)] \, ds.. \quad (6)$$

However, the second boundary problem

$$K = \kappa = \frac{3-v}{1+v}; \quad f(t) = u + iv - \frac{\partial \Xi}{\partial x} - i\frac{\partial \Xi}{\partial y}. \quad (7)$$

Where G is the shear modulus, v is Poisson's coefficient, $L(s)$ and $D(s)$ are the components of external forces specified on the boundary of the plane, and u, v are the displacement components.

The components of stress are given by; see Hetnarski and Ignaczak [19]

$$\sigma_{xx} + \sigma_{yy} = 4G\left[\Phi'(z) + \overline{\Phi'(z)} - \lambda\,\Theta\right],$$
$$\left(\lambda = \frac{\alpha}{2}(1+\nu)\right),$$

$$\sigma_{yy} - \sigma_{xx} + 2i\,\sigma_{xy} = 2G\left[\frac{\partial^2\Xi}{\partial y^2} - \frac{\partial^2\Xi}{\partial x^2} + 2i\frac{\partial^2\Xi}{\partial x\partial y}\right]$$
$$+ 4G\left[\overline{z}\,\Phi''(z) + \Psi'(z)\right], \tag{8}$$

where λ is denoted as the heat transfer coefficient.

The solution of Equation (2), when the heat is perpendicular to the plate, is given by [16]

$$\Theta = q\left(Imz + \frac{r_o^2}{Imz}\right). \tag{9}$$

Here, the function z is defined by Equation (1). Substituting from Equation (9) into Equation (3) and integrating the result, the thermoelastic potential becomes

$$\blacksquare(z) = (1+\nu)\,\alpha q r_o^2 Imz\left[\ln(z-\overline{z}) - 1\right]. \tag{10}$$

Now, from Equations (9), (10) the values of Θ and $\Xi\,(z)$ are totally resolved.

Consequently, the stress components of Equation (8) can be modified as follows:

$$\sigma_{xx} = G[-(\frac{\partial^2\Xi}{\partial y^2} - \frac{\partial^2\Xi}{\partial x^2} + 2\lambda\Theta)$$
$$+ 2Re(2\Phi'(z) - N(z,\overline{z}))],$$

$$\sigma_{yy} = G[\left(\frac{\partial^2\Xi}{\partial y^2} - \frac{\partial^2\Xi}{\partial x^2} - 2\lambda\Theta\right)$$
$$+ 2Re\left(2\Phi'(z) + N(z,\overline{z})\right)],$$

$$\sigma_{xy} = 2G\left[\frac{\partial^2\Xi}{\partial x\partial y} + ImN(z,\overline{z})\right], \tag{11}$$
$$N(z,\overline{z}) = \overline{z}\Phi''(z) + \Psi'(z).$$

After getting the Gaursat functions, the stress components are determined in their entirety.

3 The parametric equation of the conformal mapping:

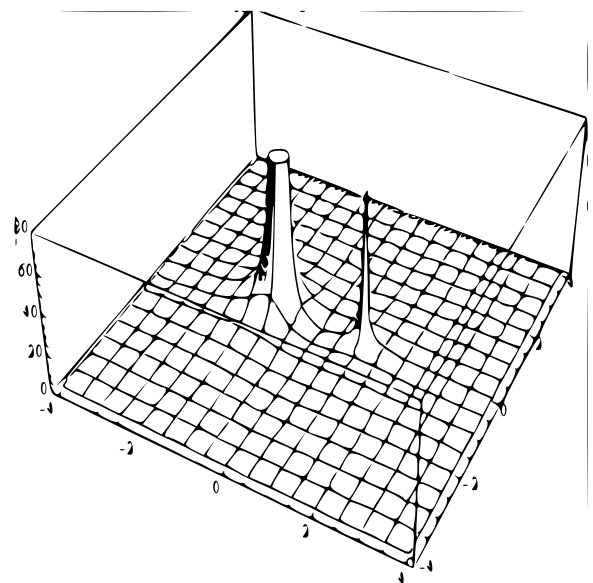The parametric equations of the rational mapping function (1) takes the form

$$x = \frac{1}{R_1^2 + R_2^2}[R_1(\ell_1 u_1^+ - \ell_2 v_1^+ + m_1 u_1^- - m_2 v_1^-)$$
$$+ R_2(\ell_1 v_1^+ + \ell_2 u_1^+ + m_2 u_1^- + m_1 v_1^-)],$$

$$y = \frac{1}{R_1^2 + R_2^2}[R_1(\ell_1 v_1^+ + \ell_2 u_1^+ + m_1 v_1^- + m_2 u_1^-)$$
$$- R_2(\ell_1 u_1^+ - \ell_2 v_1^+ - m_2 v_1^- + m_1 u_1^-)]. \tag{12}$$

where $R_1 = \sigma^2 - \xi^2 - 1 - (n_1 u_1^- - n_2 v_1^-)$, $\quad R_2 = 2\sigma\xi - (n_1 v_1^- + n_2 u_1^-)$,
$\quad u_1^\pm = (\sigma \pm 1)^2 - \xi^2, v_1^\pm = 2(\sigma \pm 1)\xi$.

In the following diagram, the plate of the singular term of the rational mapping (12) is viewed rapidly.


Fig. 1: Fig. 1 describes a fast look at the singularity of the rational mapping (12) on the plate.

The interest of the transformation (1) due to the different shapes of holes it treats (see Figs. (2)-(11)). In addition, we state the following:-:

1. The number of angles of the holes is subject to n values. They are given by $n+1$.

2. The complex constant m causes the circling shape of the symmetry situation and the circling angle is given by $\tan\theta = \frac{m_2}{m_1}, m = m_1 + im_2$. Positive values θ mean the circling will be in the anticlockwise direction and negative values will be in the clockwise direction.

3. For real values: l, m, n: Real numbers
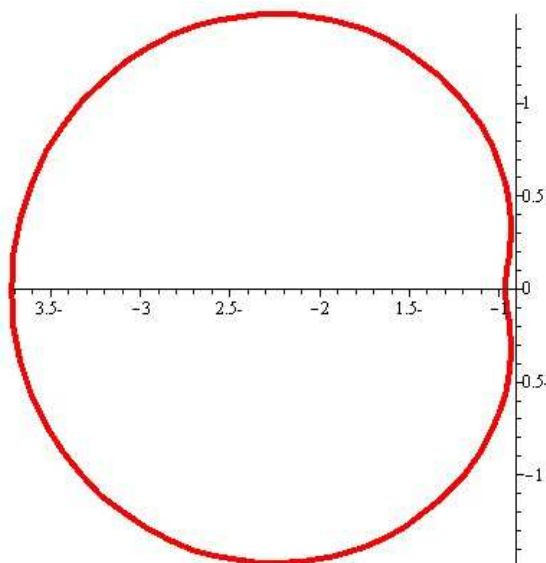
4. For complex constants

4 Gaursat functions

In this section, we use the transformation mapping (1) in the boundary value problem (4) with the aid of (5), then we apply the complex variable method with the residue
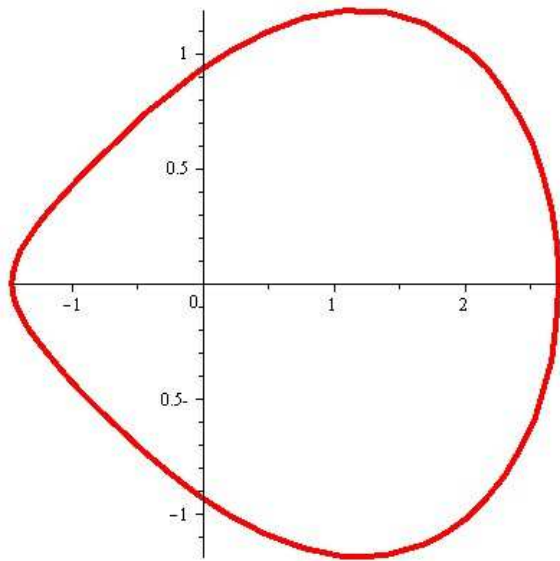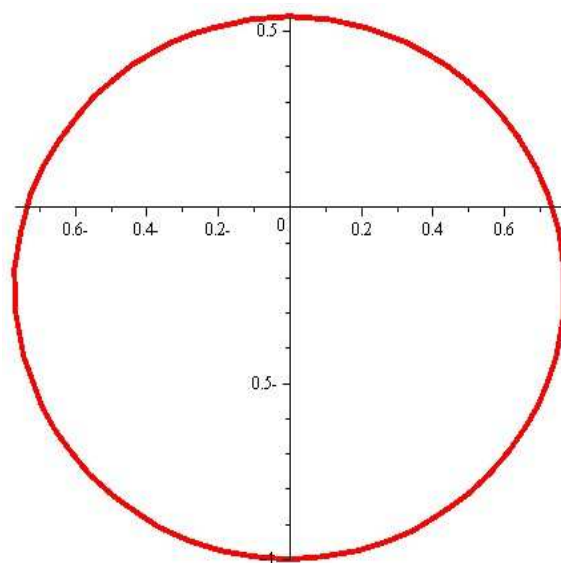
Fig. 2: $(l,m,n) = (0.5,\ 1.4,\ 0.3)$.
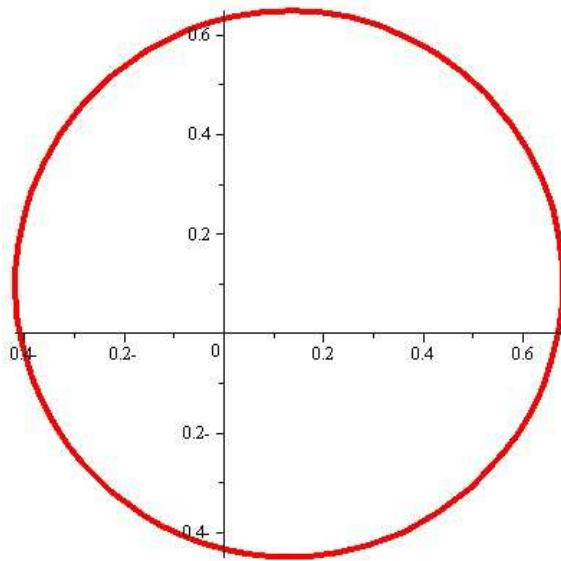
Fig. 4: $(l,m,n) = (0.00,\ 0.4 + 0.3i,\ 0.3)$.

Fig. 3: $(l,m,n) = (0.2,\ 1.3,\ 0.7)$.

Fig. 5: $(l,m,n) = (0.00,\ 0.7,\ 0.3i)$.

theorems to obtain a closed expression for Gaursat functions.

Therefore, the expression $\overline{\dfrac{\omega\,(i\xi)}{\omega'\,(i\xi)}}$ can be written in the form
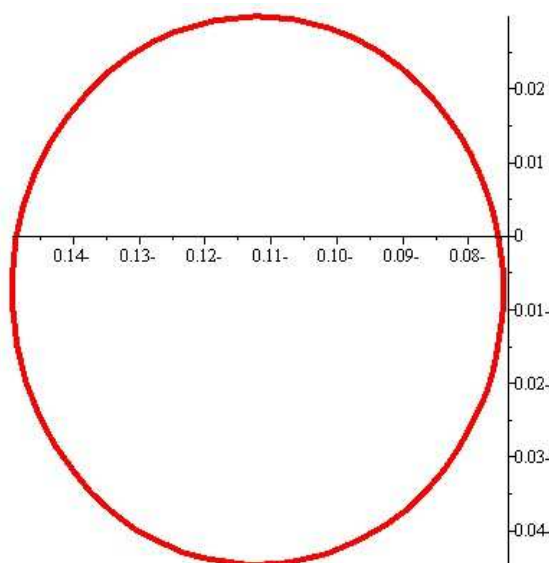
$$\overline{\frac{\omega\,(i\xi)}{\omega'\,(i\xi)}} = \overline{\alpha\,(i\xi)} + \beta\,(i\xi), \qquad (13)$$
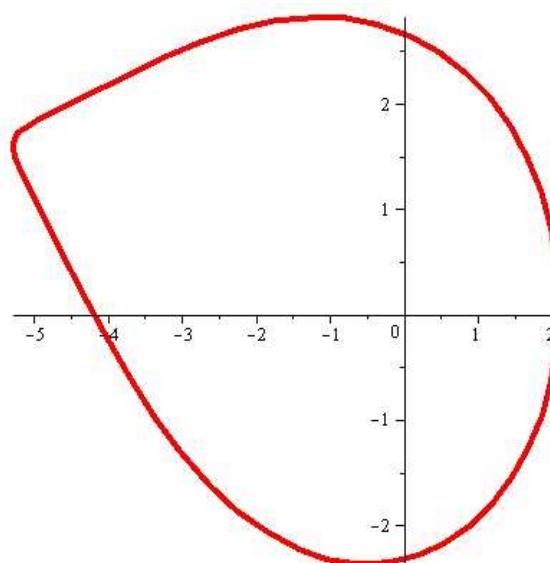
where

$$\alpha\,(i\xi) = \frac{h}{a + i\xi}, \quad a = \frac{1+n}{1-n}, |n| \neq 1,$$

$$h = \frac{-(1-\overline{n})^2}{(1-n)^2} *$$
$$\frac{16n^2\,(Rea)^2\,(m+n^2\ell)}{4n^2\overline{m}+\overline{\ell}\,(1-n)\,(1-\overline{n})\left(1+|a|^2-6Rea\right)}, \qquad (14)$$
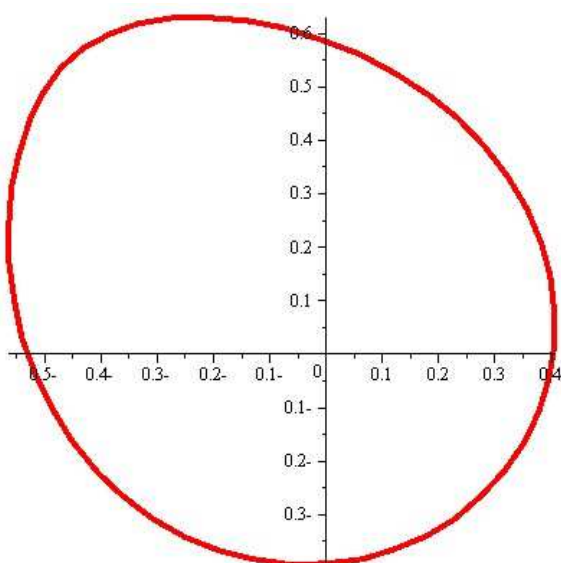
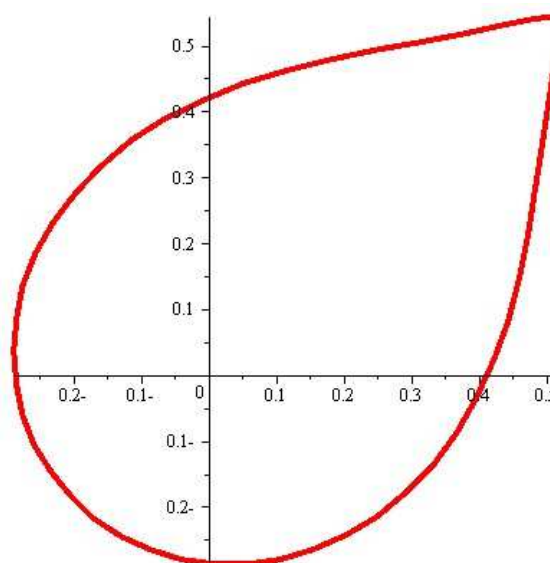and $\beta(s)$ is a regular function, region of interest is limited to the right half-plane, excluding the point at infinity.

Fig. 6: $(l,m,n) = (0.00, 0.3i, 0.2+3i)$.

Fig. 8: $(l,m,n) = (0.9+2.3i, 0.0, 0.45i)$.

Fig. 7: $(l,m,n) = (0.4+0.3i, 0.0, 3i)$.

Fig. 9: $(l,m,n) = (0.4+0.04i, 0.0, 0.35+0.4i)$.

Using (13) and (5) in (4), we get

$$K\Phi(i\xi) - \alpha(i\xi)\overline{\Phi'(i\xi)} - \overline{\Psi_*(i\xi)} = F_*(i\xi), \quad (15)$$

where

$$\Phi(i\xi) = \Phi(\omega(i\xi)), \Psi(i\xi) = \Psi(\omega(i\xi)),$$
$$\Psi_*(i\xi) = \Psi(i\xi) + \beta(i\xi)\Phi'(i\xi),$$

$$F_*(i\xi) = F(i\xi) - K\Gamma\omega(i\xi)$$
$$+ \overline{\Gamma^*}\overline{\omega(i\xi)} + \omega(i\xi)\overline{E(i\tau)},$$

$$\overline{E(i\xi)} = \overline{\Gamma} - \frac{S_x - iS_y}{2\pi(1+\kappa)}\frac{1}{\overline{\omega(i\xi)}}, \quad (16)$$
$$F(s) = F(\omega(s)).$$

The function $F(s)$ with its derivatives must satisfy the Hölder condition, and we assume that
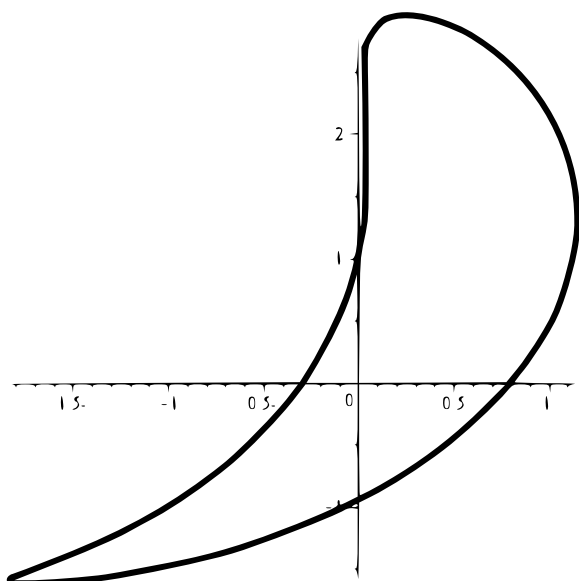$$\Phi(\infty) = \Psi(\infty) = 0.$$

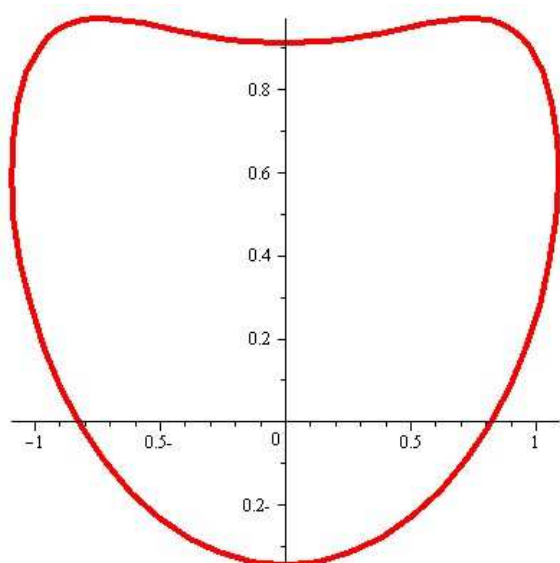**Fig. 10:** $(l, m, n) = (0.7 + 0.9i, 0.4 + 1.7i, 0.45i)$.

Fig. 11: $(l, m, n) = (0.9, 0.4, 0.45i)$.

Multiplying both sides of Equation (15) by the term $\frac{d\xi}{2\pi(s - i\xi)}$, and then integrating the result with respect to ξ from $-\infty$ to ∞, to have

$$K\Phi(s) - \frac{1}{2\pi} \int_{-\infty}^{\infty} \frac{\alpha(i\xi)\,\overline{\Phi'(i\xi)}\,d\xi}{(s - i\xi)} = \frac{1}{2\pi} \int_{-\infty}^{\infty} \frac{F_*(i\xi)\,d\xi}{(s - i\xi)}. \tag{17}$$

The second of L.H.S. of Equation (17) can be written as

$$\frac{1}{2\pi} \int_{-\infty}^{\infty} \frac{\alpha(i\xi)\,\overline{\Phi'(i\xi)}}{(s - i\xi)} d\xi = \frac{hb}{s + a}, \tag{18}$$

where b is a complex constant will be determined.
Using the formula (16) in the R.H.S. of (17), then after integrating the result and with the aid of (17), we have

$$K\Phi(s) = B(s) + \frac{H}{s + a} + \frac{hb}{s + a} - \frac{2\overline{\Gamma^*\ell}}{1 + s}, \tag{19}$$

$$H = \frac{2(n^2\ell + m)}{(1 - n)^2}(K\Gamma - \overline{\Gamma})$$
$$+ \frac{n(1 - \overline{n})(m + n^2\ell)\,Re\,a\,(S_x - iS_y)}{\pi(1 + \kappa)(\overline{m}n^2 + \overline{\ell})(1 - n)}. \tag{20}$$

Using Equation (19) in (18), the complex constant b takes the form

$$b = [K^2(a + \overline{a})^4 - h\overline{h}]^{-1}\{\overline{h}H - K(a + \overline{a})^2\overline{H}$$
$$- (a + \overline{a})^2[\overline{h}B'(-a) - K(a + \overline{a})^2\overline{B'}(-\overline{a})].$$

$$+ \overline{h}H - 2(a + \overline{a})^2\left[\frac{\overline{h\Gamma^*\ell}}{(1 + \overline{a})^2} - \frac{(a + \overline{a})^2}{(1 + a)^2}K\Gamma^*\ell\right]\} \tag{21}$$

Also, from the boundary condition (4), we obtain $\Psi(s)$ in the form

$$\Psi(s) = \overline{B(s)} - \frac{2\Gamma^*\ell}{1 + \overline{s}} + \frac{\overline{H} + \overline{hb}}{\overline{a} + \overline{s}} - \frac{\overline{\omega(s)}}{\omega'(s)}\Phi'(s)$$
$$- \Gamma^*\omega(s) + (K\overline{\Gamma} - E(s))\,\overline{\omega(s)}. \tag{22}$$

where

$$B(s) = \frac{1}{2\pi} \int_{-\infty}^{\infty} \frac{F(\xi)}{(s - i\xi)} d\xi \tag{23}$$

Hence, the Gaursat functions are completely determined.

5 Special cases

(1) In our recent mapping function (1), assume $s = \frac{\zeta + 1}{\zeta - 1}$. Hence, we have the transformation mapping

$$z = \frac{\ell\zeta + m\zeta^{-1}}{1 - n\zeta^{-1}}, |n| \neq 1, \tag{24}$$

where ℓ, m and n are complex constants.
Thereon, the Gaursat functions formulas are given by

$$K\Phi(\zeta) = B(\zeta) + \frac{(H + hb)(\zeta - 1)}{\zeta(1 + a) + (1 - a)}$$
$$- \frac{\overline{\Gamma^*\ell}(\zeta - 1)}{\zeta}, \tag{25}$$

$$\Psi\left(\zeta\right) = \overline{B\left(\zeta\right)} - \Gamma^*\ell\left(1-\zeta\right) + \frac{\left(\overline{H}+\overline{h}\overline{b}\right)\left(1-\zeta\right)}{\zeta\left(1-\overline{a}\right)+\left(1+\overline{a}\right)}$$
$$- \frac{\overline{\omega\left(\zeta\right)}}{\omega'\left(\zeta\right)}\,\Phi'\left(\zeta\right) - \Gamma^*\omega\left(\zeta\right) + \left(K\overline{\Gamma}-E\left(\zeta\right)\right)\overline{\omega\left(\zeta\right)}.$$

(26)

(2) If we substitute n = metricconverterProductID0 in0 in Equation (1), the transformation mapping takes the form

$$z = \omega\left(s\right) = \frac{\ell\left(s+1\right)^2 + m\left(s-1\right)^2}{\left(s^2-1\right)}, \qquad (27)$$

then the Gaursat functions become

$$K\Phi\left(s\right) = B\left(s\right) + \frac{H}{s+a} - \frac{2\overline{\Gamma^*\ell}}{s+1}; \left(H = 2m\left(K\Gamma-\overline{\Gamma}\right)\right),$$

(28)

$$\Psi\left(s\right) = \overline{B\left(s\right)} - \frac{2\Gamma^*\ell}{\overline{s}+1} + \frac{\overline{H}}{\overline{s}+\overline{a}} - \frac{\overline{\omega\left(s\right)}}{\omega'\left(s\right)}\,\Phi'\left(s\right)$$
$$- \Gamma^*\omega\left(s\right) + \left(K\overline{\Gamma}-E\left(s\right)\right)\overline{\omega\left(s\right)}.$$

(29)

(3) If we substitute m = metricconverterProductID0 in0 in Equation (1), we get

$$z = \omega\left(s\right) = \frac{\ell\left(s+1\right)^2}{\left(s^2-1\right)-n\left(s-1\right)^2}. \qquad (30)$$

Hence, the Gaursat functions take the form

$$K\Phi\left(s\right) = B\left(s\right) + \frac{H}{s+a} + \frac{hb}{s+a} - \frac{2\overline{\Gamma^*\ell}}{s+1}, \qquad (31)$$

$$\Psi\left(s\right) = \overline{B\left(s\right)} - \frac{2\Gamma^*\ell}{1+\overline{s}} + \frac{\overline{H}+\overline{h}\overline{b}}{\overline{a}+\overline{s}} - \frac{\overline{\omega\left(s\right)}}{\omega'\left(s\right)}\,\Phi'\left(s\right)$$
$$- \Gamma^*\omega\left(s\right) + \left(K\overline{\Gamma}-E\left(s\right)\right)\overline{\omega\left(s\right)},$$

(32)

where

$$H = n^2\ell\left[\frac{2\left(K\Gamma-\overline{\Gamma}\right)}{\left(1-n\right)^2} + \frac{n\left(1-\overline{n}\right)Re\,a\left(S_x-iS_y\right)}{\pi\left(1+\chi\right)\left(1-n\right)\overline{\ell}}\right];$$
$$h = \frac{16n^4\ell\left(Re\,a\right)^2\left(1-\overline{n}\right)}{\overline{\ell}\left(1-n\right)^3\left(6\,Re\,a-|a|^2-1\right)}.$$

6 Applications

1. When the external force is applied to the central region of the curvilinear hole:

For the second boundary problem, we let $\Gamma = \Gamma^* = F = 0$, $K = \kappa$.. It is assumed that stresses disappear at infinity. The Gaurst capabilities become

$$\Phi\left(s\right) = \frac{1}{\kappa}\left(\frac{H}{s+a} + \frac{hb}{s+a}\right), \qquad (33)$$

$$\Psi\left(s\right) = \frac{\overline{H}+\overline{h}\overline{b}}{\overline{s}+\overline{a}} - \frac{\overline{\omega\left(s\right)}}{\omega'\left(s\right)}\,\varphi'\left(s\right) + \overline{\omega\left(s\right)}E\left(s\right),$$
$$\left[E\left(s\right) = \frac{S_x+iS_y}{2\pi\omega\left(s\right)\left(1+\kappa\right)}\right].$$

(34)

Where the complex constants H is calculated using Equation (20). While the complex constant b can be calculated from (21). The two constants were evaluated by using Maple 18. For m = 20+0.5i, n = 0.055+0.0025i, ℓ= 30-0.9i , κ = 2 and $S_x = S_y$ = 10. There is a connection between the components of stress σ_{xx}, σ_{yy} , σ_{xy} and σ and τ are considered in Figs. (12)-(15).
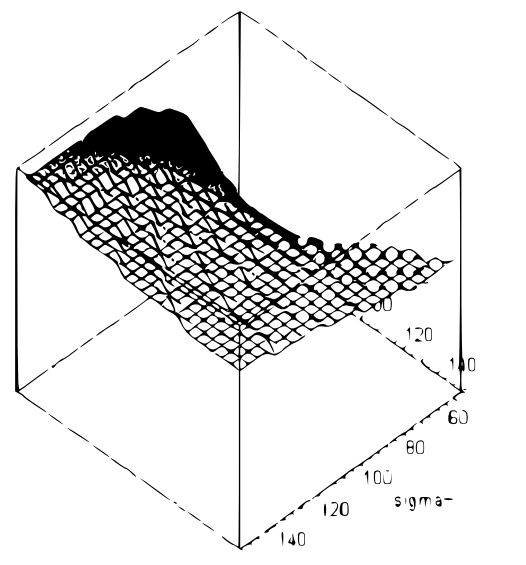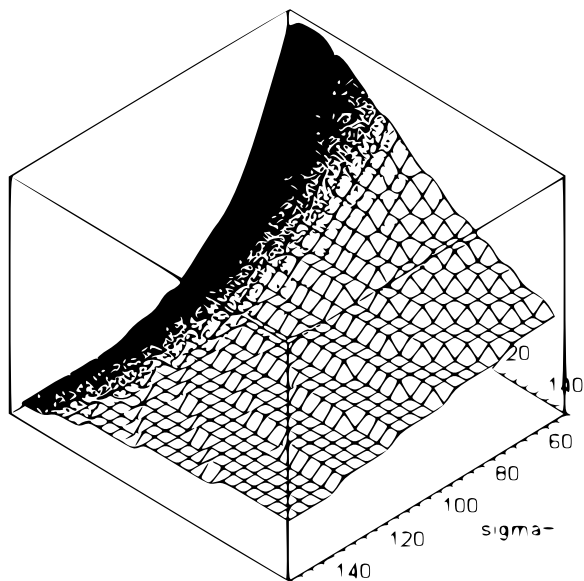

Fig. 12: Max. Value of σ_{xx} is [98.73713, [σ = 146.92700, ξ= 50.]], Min. value of σ_{xx} is[98.73697, [σ = 50, ξ = 58.84021]]

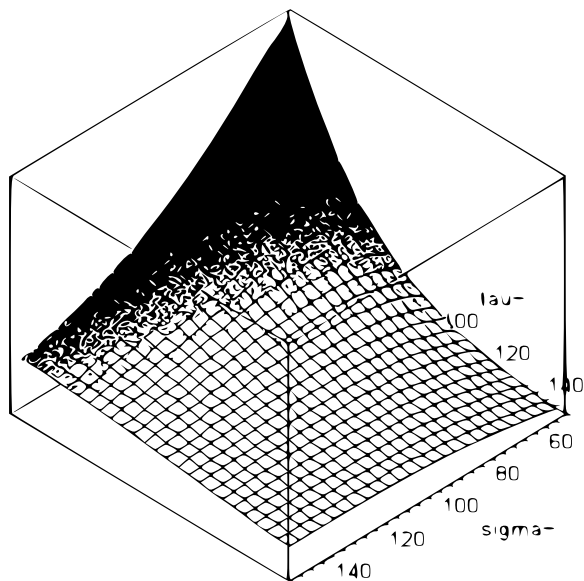2. Curvilinear slit for an infinite plate under constant tension:

For $K = -1$, Γ = P/4 , $\Gamma^* = -\frac{1}{2}Pe^{-2i\vartheta}$ and $S_x = S_y = F = 0$, the uniform tensile stress of intensity P is applied to an infinite plate at an angle to the x-axis, causing the plate to stretch to infinity. A stress-free hole C in the shape of a curve weakens the plate.
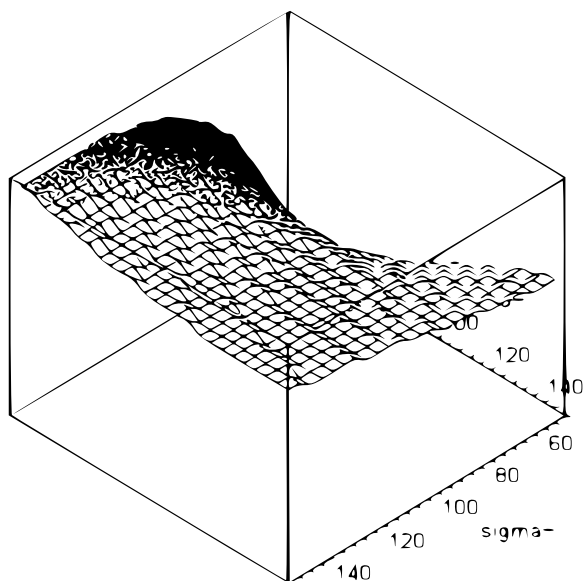
The Gaursat's operations are shaped like

$$\Phi\left(s\right) = \frac{2\overline{\ell}\overline{\Gamma^*}}{1+s} - \frac{H}{s+a} - \frac{hb}{s+a}, \qquad (35)$$

Fig. 13: Max. Value of σ_{xx} is [98.73713, [σ = 146.92700, ξ= 50.]], Min. value of σ_{xx} is[98.73697, [σ = 50, ξ = 58.84021]].
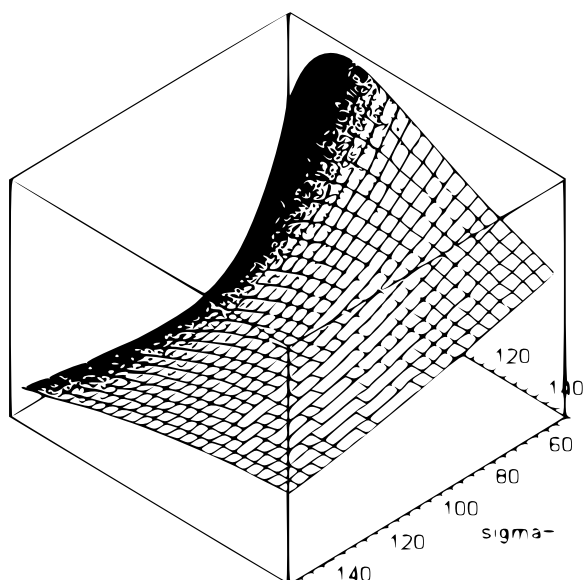

Fig. 15: Min. value of σ_{xy} is [0.000001, [σ = 50., ξ= 150.]]

P = 1/4, $\vartheta = \pi$ /4, and $S_x = S_y$ = 10. The relationship between the components of stress σ_{xx} , σ_{yy} , σ_{xy} and σ and τ are regarded in Figs. (16)-(19).

Fig. 14: Max. value of σ_{xy} is [0.00021, [σ = 50., ξ= 50.]]

$$\Psi(s) = \left(\frac{1}{2} \, \omega(s) + \frac{\ell}{1+\overline{s}} \right) P \, e^{-2i\vartheta}$$
$$+ \frac{\overline{H} + \overline{h}\overline{b}}{\overline{s} + \overline{a}} - \frac{\overline{\omega(s)}}{\omega'(s)} \Phi'(s) - \frac{1}{2} P \overline{\omega(s)}. \tag{36}$$

Where H and b are complex constants whose values were derived with Maple 18 according to Equations (20) and (21). For m = 20 + 0.5i, n = 0.055 + 0.0025i, ℓ= 30 - 0.9i,
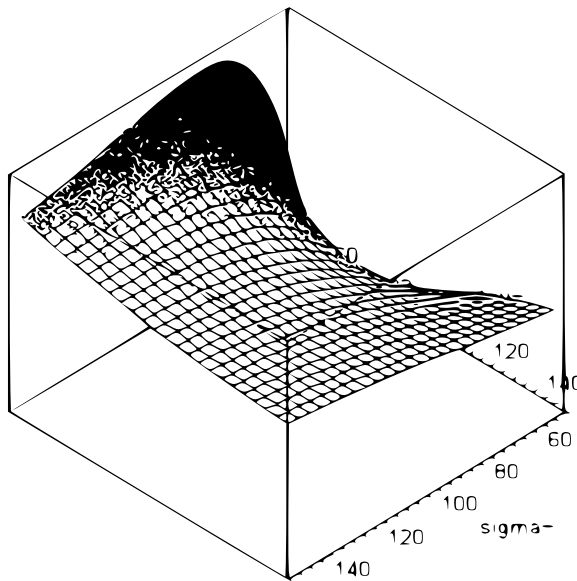

Fig. 16: Max.value of σ_{xx} is [98.75364, [σ = 50., ξ = 72.66509]], Min. value of σ_{xx} is [98.72996, [σ = 93.14166, ξ = 50.]]

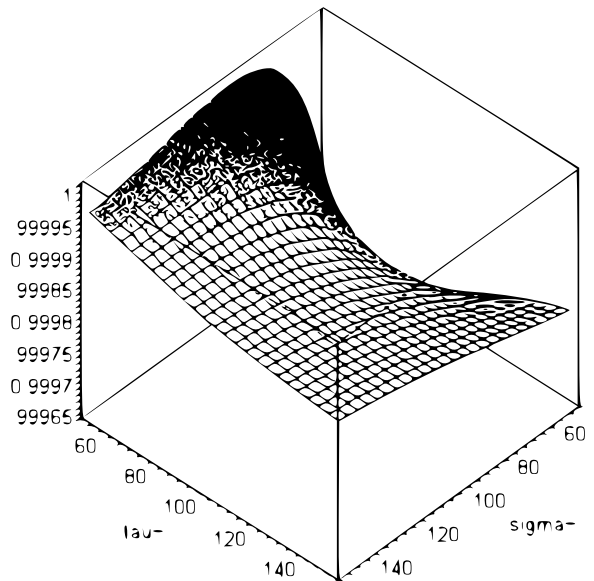**Fig. 17:** Max value of σ_{yy} is [98.73093].

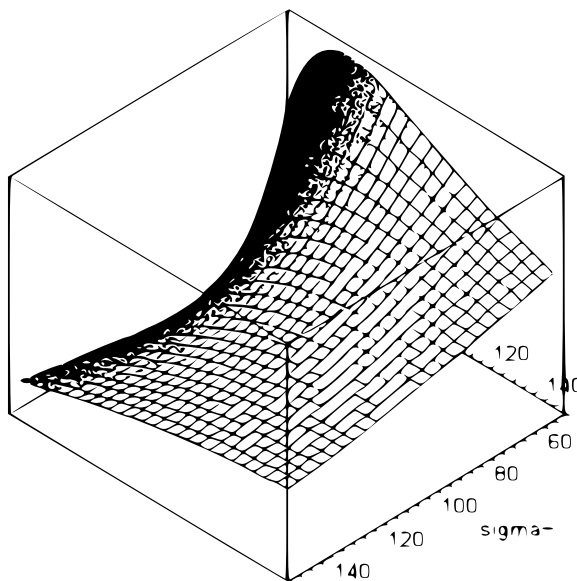**Fig. 19:** Minimum value of σ_{xy-} is [-0.03397].

Fig. 18: Maximum value of σ_{xy-} is [-0.00251].

7 The relation between S-plane and zeta-plane

In this section, we consider the relation between S- plane and ζ- plane as the following:

(1) The conformal mapping $z = c\omega(s)$, $c > 0$, $s = \sigma + i\xi$ transforms the domain of the plate with a curvilinear hole C into the domain of the right half-plane. While the mapping $z = c\omega(\zeta)$, $c > 0$, $\zeta = \rho e^{i\theta} = \varsigma + i\eta$ mapped the domain of the plate with a curvilinear hole into the domain outside $|\zeta| > 1$, or inside $|\zeta| < 1$.

(2) The transformation $s = \frac{\zeta+1}{\zeta-1}$, transforms the domain of the right half-plane into the domain outside a unit circle. The inverse case can be obtained by using the transformation $\zeta = \frac{s+1}{s-1}$.

(3) The physical desire of the discussed mappings comes from the different shapes of holes they address and the different directions they take. These mapping functions deal with famous shapes of tunnels; therefore, it is beneficial to use them in studying stresses and strains around tunnels. In underground engineering, the tunnel is assumed to be propelled in a homogeneous, isotropic, linear, elastic, and pre-stressed geometrical situation.

(3) Using the transformation $s = \frac{\zeta+1}{\zeta-1}$ in, we have the conformal mapping

$$z = \frac{\ell\zeta + m\zeta^{-1}}{1 - n\zeta^{-1}}. \qquad (37)$$

This map conforms to the curvilinear hole for the first and second boundary problems outside the unit circle γ. Write the mapping (37) in the form

$$z = n\ell + \ell\zeta + (m + n^2\ell)\sum_{r=1}^{\infty} n^{r-1}\zeta^{-r}. \qquad (38)$$

Many special cases can be obtained from the rational mapping for different values
Of ℓ, m, n especially when $m = 0, n = 0, m + \ell n^2 = 0$.

Using the transformation $s = \frac{1+\zeta}{1-\zeta}$ in (11), we have the mapping

$$z = \frac{\ell\zeta^{-1} + m\zeta}{1 - n\zeta}. \qquad (39)$$

This map confirms the curvilinear hole for the first and second boundary problems inside the unit circle γ. Write in the form

$$z - \ell n = \frac{\ell}{\zeta} + (m + \ell n^2)\zeta \sum_{\alpha=0}^{\infty} n^\alpha \zeta^\alpha.$$

If we put m = 0 and then ignore the constant term with assuming the constants $n^{\alpha-1} = 0, \quad for \ \alpha = 3$, we have the rational mapping function

$$z = \ell(\zeta^{-1} + \sum_{\alpha=1}^{3} n^{\alpha+1}\zeta^\alpha). \tag{40}$$

The Gaursat functions according to using the mapping (40) are equivalent to the forms found by Exadaktylos and Stavropoulou [9]. In addition, for the conformal mapping of Equation (39), if we put $m = 0$ and then ignore the constant term by assuming the constants $n^{2\alpha-1} = 0, \ 1 \le \alpha \le r < \infty$ where $r < \infty$ we have the mapping function $z = \ell(\zeta^{-1} + \sum_{\alpha=1}^{r} n^{2\alpha+1}\zeta^{2\alpha-1})$, by eliminating the elements after r. The Gaursat functions, according to these modifications, are equivalent to the forms found by Exadaktylos, Liolios, and Stavropoulos [10].

8 General Conclusions:

From all previous sections, we can establish the following:-

(1) Complex plane: Many ethereal phenomena exist in nature, such as magnetic fields, electricity, and heat. Therefore, in the real plane, these phenomena cannot be explained mathematically. For this, the complex plane plays an important role in presenting these intangibles and explaining their phenomena.

(2) In addition, with the rapid development of science, many mathematical problems that cannot be solved at the real level, find that their solutions can be discussed at the complex level. So we find that the first to use complex function theory methods in two-dimensional problems of elasticity was N.I. Muskhelishvili, see Muskhelishvili [19].

(3) In the two-dimensional linear elasticity theory, graphs play a prominent role as one of the most effective ways to solve the problem of the boundary value of a region weakened by a curved hole in transforming the region into a simplified form in order to obtain problem-free solutions. These different symbols help transform very complex shapes into simple shapes. It also allows basic complex variable modulation to be extended to the transformation problem, making robust methods for finite solutions of circular and semi-plane regions applicable to these problems.

References

[1] S. Kumar and V. Gupta. An approach based on fractional-order Lagrange polynomials for the numerical approximation of fractional-order non-linear Volterra-Fredholm integro-differential equations. Journal of Applied Mathematics and Computing. **69**, 251-272 (2023).

[2] S. Zachariah, S. Shenoy, D. Pai, Experimental analysis of the effect of the woven aramid fabric on the strain to failure behavior of plain weaved carbon/aramid hybrid laminates, Facta Univ. Ser. Mech., in press. https://doi.org/0.22190/FUME200819022Z

[3] C. Gonenli, O. Das, Free vibration analysis of circular and annular thin plates based on crack characteristics, Reports in Mechanical Engineering **3**, 158-167 (2022). https://doi.org/10.31181/rme20016032022g

[4] A. Lal, M. Vaghela, K. Mishra, Numerical analysis of an edge crack isotropic plate with void/inclusions under different loading by implementing XFEM, J. Appl. Comput. Mech. **7**, 1362-1382 (2021). https://doi.org/10.22055/jacm.2019.31268.1848

[5] N. Duruk, H. Erbay, A. Erkip, Global existence and blow-up for a class of nonlocal nonlinear Cauchy problems arising in elasticity, Nonlinearity **23**, 107-118 (2010). http://dx.doi.org/10.1088/0951-7715/23/1/006

[6] A. R. Jan, An Asymptotic model for solving mixed integral equation in position and time, Journal of Mathematics **2022**, Article ID 8063971, 1-11 (2022). https://doi.org/10.1155/2022/8063971

[7] M. Abdou, S. Raad, S. AlHazmi, Fundamental contact problem and singular mixed integral equation, Life Sci. J. **11**, 323-329 (2014).

[8] M. Abdou, A. Jan, On a computational method for solving nonlinear mixed integral equation with singular kernel, J. Comput. Theor. Nanos. **13**, 2917-2923 (2016). https://doi.org/10.1166/jctn.2016.4938

[9] G. E. Exadaktylos, M.C. Stavropoulou, A closed-form elastic solution for stress and displacement around tunnels, Int. J. Rock Mech. Min. **39**, 905-916 (2002). https://doi.org/10.1016/S1365-1609(02)00079-5

[10] G. E. Exadaktylos, P. A. Liolios, M. C. Stavropoulou, A semi-analytical elastic stress-displacement solution for notched circular openings in rocks, Inter. J. of solids and structures **40**, 1165-1167 (2003).

[11] A. Lu, Z. Xu, N. Zhang, Stress analytical solution for an infinite plane containing two holes, Int. J. Mech. Sci. **128**, 224-234 (2017). https://doi.org/10.1016/j.ijmecsci.2017.04.025

[12] M. Abdou, Fundamental problems for infinite plate with a curvilinear hole having finite poles, Appl. Math. Comput. **125**, 79-91 (2002). https://doi.org/10.1016/S0096-3003(00)00117-X

[13] M. Abdou, S. Asseri, Gaursat functions for an infinite plate with a generalized curvilinear hole in zeta plane, Appl. Math. Comput. **212**, 23-36 (2009). http://dx.doi.org/10.1016/j.amc.2009.01.079

[14] M. A. Abdou, S. A. Asseri, Gaursat functions for an infinite plate with a generalized curvilinear hole in Zeta-plane, J. Appl. Math. Comput. **212**, 23-36 (2009).

[15] X. Zeng, A. Lu, N. Zhang, Analytical stress solution for an infinite plate containing two oval

holes, Eur. J. Mech. A-Solid. **67**, 291-304, (2018). https://doi.org/10.1016/j.euromechsol.2017.09.011

[16] M. Abdou, M. Basseem, Thermopotential function in position and time for a plate weakened by curvilinear hole, Arch. Appl. Mech. **92**, 867-883 (2022). https://doi.org/10.1007/s00419-021-02078-x

[17] Sharifah E. Alhazmi, M. A. Abdou and M. Basseem, The stresses components in position and time of weakened plate with two holes conformally mapped into a unit circle by a conformal mapping with complex constant coefficients, AIMS Mathematics **8(5)**, 11095-11112 (2023).

[18] H. Parkus, Thermoelectricity, Springer Verlag, New York, 1975.

[19] R.B. Hetnarski, J. Ignaczak, Mathematical Theory of Elasticity, Taylor and Francis, 2004.

[20] N. I. Muskhelishvili, Some Basic Problems of Mathematical Theory of Elasticity, fifth Ed. Noordhoof, Netherland, 1985.

Azhar R. A. Jan received a PhD degree in Applied mathematics-elasticity at Alexandria University in Egypt. His research interests are in the areas of applied mathematics, and mathematical physics including mathematical methods and Elasticity, Fluid, and integral equations. He has published research articles in reputed international journals of mathematical and engineering sciences. He is the referee and editor of mathematical journals.